*Exp. Theo. NANOTECHNOLOGY* 10 (2026) 965-978 https://doi.org/10.56053/10.S.965

# A dual-action nanocoating system for corrosion and microbial protection of Mg-AZ31 Alloy: Towards a new generation of smart orthopedic implants with advanced nanotechnology-driven biointerfaces

*Aya Kahled Jabbar*[1], *Hussein Ali Hussein*[1,*], *M. Al Nuaimi*[2]

[1]Production Engineering, and Metallurgy College, University of Technology- Iraq, Baghdad, Iraq
[2]College of Applied Sciences, University of Technology-Iraq, Baghdad, Iraq
[*]) Email: Hussein.A.Aldaffaie@uotechnology.edu.iq

*Received* 7/2/2026, *Received in revised form* 17/4/2026, *Accepted* 26/4/2026, *Published* 15/5/2026

---

This study reports the development of a smart dual-action nanocoating system for enhancing the corrosion resistance and antimicrobial performance of Mg-AZ31 alloy for orthopedic implant applications. FTIR analysis confirmed successful cross-linking of the polymeric network, with a characteristic carbonyl peak at 1716 $cm^{-1}$, indicating the formation of a stable encapsulation matrix. FE-SEM revealed nanocapsules with sizes ranging from 46.2 to 305.7 nm, forming a dense "cauliflower-like" structure with finer features down to 28.64 nm, promoting surface roughness and bioactivity. Electrochemical evaluation demonstrated a significant shift in corrosion potential from approximately −700 mV (bare alloy) to −260 mV for coated samples, achieving a high corrosion protection efficiency of 93.75%. Antibacterial testing using Zone of Inhibition (ZOI) assays showed strong inhibitory effects against *Staphylococcus aureus*, effectively preventing biofilm formation. EDX analysis confirmed hydroxyapatite formation with an ideal Ca/P ratio of 1.67, indicating excellent bioactivity. The coating also exhibited superior adhesion, classified as 5B according to ASTM standards, with no observable peeling. These results demonstrate that the developed nanocoating provides synchronized corrosion protection, antimicrobial activity, and biointegration, offering a promising strategy for next-generation biodegradable orthopedic implants. Furthermore, advanced nanotechnology design enables controlled drug release, nanoscale surface tuning, and intelligent responsiveness to physiological stimuli, significantly enhancing implant performance and long-term stability.

**Keywords:** Smart nanocapsules; Complex coacervation; Corrosion inhibition; Antimicrobial.

## 1. INTRODUCTION

Magnesium (Mg) and its alloys, particularly Mg-AZ31, have emerged as promising materials for biodegradable orthopedic implants due to their excellent biocompatibility, suitable mechanical properties, and ability to degrade naturally within the human body [1-3]. Unlike traditional metallic implants, magnesium-based systems can gradually dissolve after fulfilling their mechanical function, thereby eliminating the need for secondary surgical removal [4,5]. In addition, magnesium ions play a beneficial role in stimulating bone growth and enhancing osteointegration [6,7]. These advantages position Mg-AZ31 as a strong candidate for next-generation biomedical implants that aim to integrate seamlessly with biological tissues while supporting the natural healing process [8,9]. However, the clinical application of Mg-AZ31 alloys is significantly hindered by their high chemical reactivity in physiological environments [10,11]. The alloy undergoes rapid corrosion when exposed to body fluids, leading to premature degradation, excessive hydrogen gas evolution, and localized alkalization [12,13]. These effects can compromise the mechanical stability of the implant and negatively impact surrounding tissues. Furthermore, the implant surface is highly susceptible to bacterial colonization, which can result in biofilm formation and post-surgical infections [14,15]. These combined electrochemical and biological challenges represent critical barriers to the widespread use of magnesium-based implants in orthopedic applications [16-20]. To address these issues, various surface modification techniques have been explored, including polymer coatings, ceramic layers, and corrosion inhibitors. While these strategies have shown some success, most approaches focus on either improving corrosion resistance or enhancing antimicrobial activity independently, without achieving a synergistic effect. Additionally, many conventional coatings are passive in nature and lack the ability to respond dynamically to changes in the physiological environment, such as fluctuations in pH caused by corrosion or microbial activity. This limitation reduces their effectiveness over time and highlights the need for more advanced, multifunctional coating systems.

Recent advancements in nanotechnology have opened new pathways for the development of smart, stimuli-responsive coatings capable of addressing multiple challenges simultaneously. In particular, nanocapsule-based systems fabricated through complex coacervation offer the ability to encapsulate functional agents and release them in a controlled manner in response to environmental triggers. By integrating corrosion inhibitors and antimicrobial nanoparticles within a polymeric matrix, it becomes possible to design coatings that provide both chemical protection and biological defense. Moreover, engineered nano-topographies can mimic natural bone structures, promoting cell adhesion and facilitating hydroxyapatite formation, which is essential for successful osseointegration. Despite these advances, there remains a significant research gap in the development of integrated systems that combine corrosion control, antimicrobial functionality, and bioactivity within a single smart coating. Existing solutions often lack responsiveness, long-term stability, or the ability to synchronize degradation with the bone healing process. Therefore, a comprehensive approach that unifies these functionalities into a single platform is essential for achieving reliable and clinically viable magnesium-based implants. Recent progress in nanotechnology has enabled the development of multifunctional smart coatings capable of responding dynamically to physiological conditions. Nanoscale engineering allows precise control over surface morphology, chemical functionality, and release kinetics of active agents. These advancements contribute to improved corrosion resistance, enhanced antibacterial performance, and superior biointegration in biomedical implants, making

nanotechnology a key driver in next-generation implant design. In this paper, a dual-action, stimuli-responsive nanocoating system is developed for Mg-AZ31 alloy to overcome the limitations of conventional surface treatments. The proposed coating is based on complex coacervation of natural polymers, incorporating 2-mercaptobenzothiazole (MBT) as a corrosion inhibitor and silver nanoparticles (AgNPs) as antimicrobial agents within nanocapsules. The coating is applied using a dip-coating technique to form a uniform and bioactive nano-interface with a characteristic "cauliflower-like" morphology. Comprehensive characterization is performed using FTIR, FE-SEM, electrochemical Tafel analysis, antibacterial Zone of Inhibition tests, and EDX analysis. The study aims to demonstrate that the developed system can achieve synchronized corrosion protection, antimicrobial activity, and enhanced biointegration, paving the way for a new generation of smart biodegradable orthopedic implants.

## 2. EXPERIMENTAL METHODOLOGY AND PROCEDURAL FRAMEWORK

### *2.1. Substrate preparation and surface engineering of Mg-AZ31 alloy*

The experimental sequence commences with the rigorous selection and preparation of Mg-AZ31 magnesium alloy substrates. This specific alloy is chosen due to its optimized elemental composition, featuring 3% Aluminum and 1% Zinc, which provides a superior balance between mechanical integrity and degradation kinetics. The mechanical preparation phase is a critical determinant of the subsequent coating adhesion and long-term stability. The alloy is sectioned into standardized coupons and subjected to a systematic, progressive grinding process using Silicon Carbide (SiC) abrasive papers, ranging from 600 to 2000 grit. This meticulous gradation is designed to eliminate irregular natural oxide layers and create a homeostatic, mechanically uniform surface. Following the grinding phase, the coupons undergo Ultrasonic Cleaning in high-purity ethanol for 15 minutes to eradicate any microscopic debris, residual lubricants, or organic contaminants. Finally, the substrates are dried using a warm air stream to ensure a chemically active and pristine surface, ready for the deposition of the functional nano-layers.

### *2.2. Nanocapsule synthesis via complex coacervation technology*

The synthesis of intelligent nanocapsules constitutes the functional core of this methodology. This process leverages the phenomenon of Complex Coacervation, driven by the electrostatic attraction between two oppositely charged biopolymers: Gelatin (the cationic agent) and Gum Arabic (the anionic agent). These polymers are dissolved in deionized water under strictly controlled thermal conditions (approximately 50°C) to ensure the complete solvation and mobility of the polymeric chains. Subsequently, the "functional payload," consisting of the corrosion inhibitor MBT and Silver Nanoparticles (AgNPs), is introduced via high-speed emulsification to create a stable oil-in-water or solid-in-water suspension. The critical success factor in this step is the precise modulation of the pH to reach the "isoelectric point" where maximum polymer interaction occurs, leading to the phase separation and deposition of the polymeric shell around the active agents. To ensure the structural robustness of these capsules and prevent premature degradation, Glutaraldehyde is introduced as a Cross-linking agent. This chemical bridging transforms the fragile coacervate shell into a rigid, chemically stable, and stimuli-responsive nanostructure.

### *2.3. Advanced surface coating and bio-interface engineering*

Upon the stabilization of the nanocapsule suspension, it is integrated into a water-borne epoxy resin matrix at meticulously calibrated concentrations (e.g., 0.1, 0.2, and 0.3 wt% of AgNPs) to formulate a

"Smart Hybrid Coating." The coating is applied to the prepared magnesium substrates utilizing the Dip-coating technique at a constant and controlled withdrawal speed. This technique is specifically chosen to ensure the deposition of a thin, homogeneous, and reproducible film across the complex geometry of the potential implant. The coated specimens then undergo a controlled thermal Curing process at low temperatures to preserve the bioactivity of the encapsulated agents while ensuring the mechanical cross-linking of the resin matrix. This process results in the formation of the "cauliflower-like" nanotopography observed via electron microscopy—a surface specifically engineered to maximize the available surface area for subsequent osteoblast attachment and biomineralization.

### *2.4. Analytical protocols for electrochemical and biological characterization*

To validate the performance of the engineered system, the specimens are subjected to a rigorous battery of analytical tests. First, Fourier Transform Infrared Spectroscopy (FTIR) is utilized to analyze molecular vibrations and confirm the success of the chemical cross-linking within the polymeric shell. Second, the defensive performance against corrosion is evaluated using Potentiodynamic Polarization (Tafel Analysis) in a Simulated Body Fluid (SBF) medium at a physiological temperature of 37°C. By measuring the corrosion current ($I_{corr}$) and corrosion potential ($E_{corr}$), the protection efficiency is quantitatively determined. Third, Zone of Inhibition (ZOI) assays are conducted to assess the antimicrobial potency against *Staphylococcus aureus*, providing proof of the proactive biological defense. Finally, a long-term immersion study in SBF is performed to evaluate the surface's ability to stimulate Hydroxyapatite growth, which is definitively confirmed through Energy-Dispersive X-ray Spectroscopy (EDX) by monitoring the characteristic Calcium (Ca) and Phosphorus (P) peaks.

### *2.5. Nanotechnology optimization strategy*

Advanced nanotechnology strategies are considered to optimize coating performance, including nanoscale tuning of capsule size distribution, controlled nanoparticle dispersion, and enhancement of interfacial bonding between the polymer matrix and the Mg-AZ31 substrate. These approaches improve coating uniformity, increase barrier properties, and enable more efficient stimuli-responsive release mechanisms under physiological conditions.

## 3. RESULTS AND DISCUSSION

### *3.1. Comprehensive interpretation of FTIR spectra*

The successful synthesis and chemical integration of the smart nanocoating on the Mg-AZ31 substrate are confirmed using Fourier Transform Infrared Spectroscopy (FTIR). As illustrated in Figure 1, a comparative analysis between the baseline polymer (PETNH) and the loaded smart system (PETNH-CuAg) reveals significant spectral shifts and the appearance of new functional groups. These changes clearly indicate the successful encapsulation of active agents and the formation of a cross-linked polymeric network, validating the effectiveness of the complex coacervation process and the stability of the developed coating system [21-25]. In the hydroxyl and amine region (3600–3000 $cm^{-1}$), a broad and intense absorption band centered at 3289 $cm^{-1}$ is observed, which is characteristic of strong hydrogen bonding interactions within the gelatin and gum arabic matrix. Additional peaks at 3529 $cm^{-1}$ and 3417 $cm^{-1}$ correspond to the stretching vibrations of free and bound hydroxyl (–OH) groups and primary amine ($–NH_2$) groups. The broad nature of this region reflects the formation of an extensive hydrogen-bonding network, which plays a critical role in the coating’s stimuli-responsive behavior. In physiological environments, fluctuations in pH—arising from magnesium corrosion or bacterial metabolic activity—can disrupt these hydrogen bonds, thereby acting as a molecular trigger

for the controlled release of encapsulated corrosion inhibitors and silver nanoparticles [26-30]. The aliphatic C–H stretching region (3000–2800 $cm^{-1}$) exhibits distinct peaks at 2997, 2973, 2926, and 2849 $cm^{-1}$, corresponding to the asymmetric and symmetric stretching vibrations of C–H groups within the polymer backbone. The presence and sharpness of these peaks confirm that the hydrocarbon chains of the gelatin/gum arabic matrix remained chemically intact during the nanocapsule synthesis process. This preservation of the polymer structure is essential for maintaining the mechanical integrity and durability of the protective coating layer [31,32]. The carbonyl and fingerprint region (1800–1200 $cm^{-1}$) provides critical evidence for the cross-linking mechanism and the successful incorporation of functional components. A strong and sharp peak at 1716 $cm^{-1}$ is attributed to the C=O stretching vibration of ester or amide groups, confirming the formation of chemical bridges between glutaraldehyde and the polymer chains. This cross-linking transforms the coating from a soluble system into a stable, water-resistant bio-interface. Additionally, the characteristic Amide I and Amide II bands at 1681, 1657, and 1566 $cm^{-1}$ represent the protein structure of gelatin. The slight shifts observed in these peaks after the incorporation of CuAg nanoparticles suggest coordination interactions between the metallic particles and the nitrogen and oxygen atoms of the polymer matrix, indicating that the nanoparticles are chemically stabilized rather than merely physically entrapped [33]. Furthermore, peaks observed at 1244 $cm^{-1}$ and 1341 $cm^{-1}$ are associated with C–O stretching vibrations and possible S=O functional groups originating from the MBT (2-mercaptobenzothiazole) corrosion inhibitor. The presence of these peaks confirms the successful encapsulation of the inhibitor within the nanocapsules. Overall, the FTIR analysis provides strong evidence of the formation of a chemically integrated, cross-linked, and functional smart coating system capable of delivering both corrosion protection and antimicrobial activity [34].

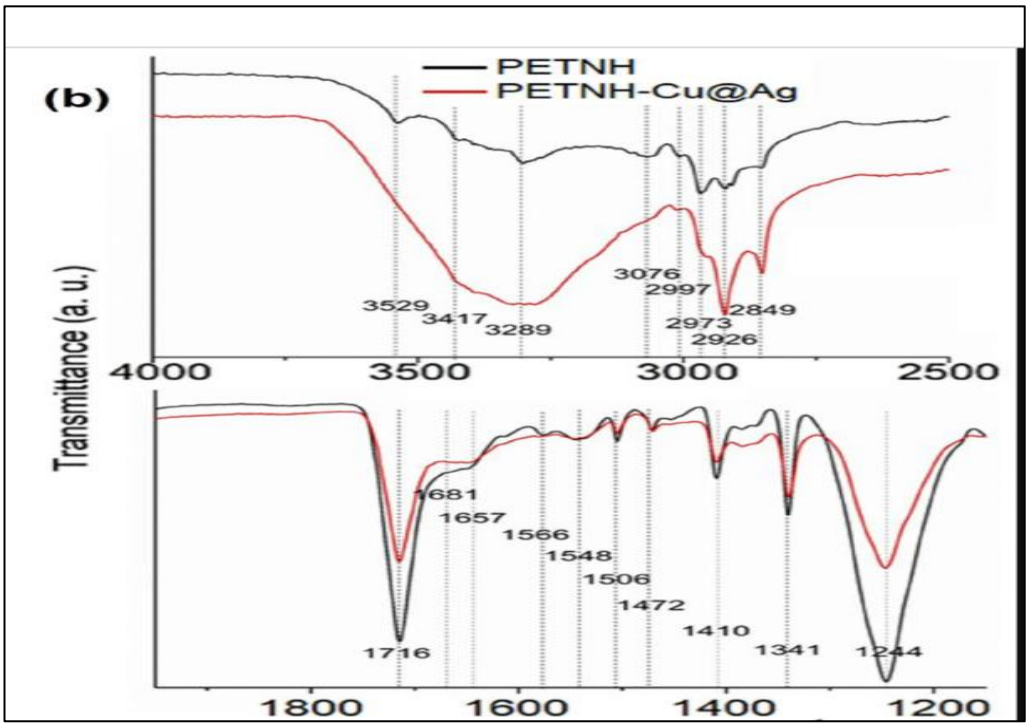


**Figure 1** FTIR spectra of samples exposed to different environmental sites (Seaside and Desert), demonstrating the chemical bond stability at 1716 $cm^{-1}$ and 3289 $cm^{-1}$ over time.

### *3.2. Scanning electron microscopy (FE-SEM)*

The field emission scanning electron microscopy (FE-SEM) micrographs presented in Fig 2. (A), (B), and (C) reveal a sophisticated structural evolution at the smart coating interface of the Mg-AZ31 magnesium substrate. Figure 2 (A) illustrates the presence of discrete spherical nanocapsules with a size distribution ranging from 46.2 nm to larger capsules reaching 305.7 nm, which definitively validates the success of the Complex Coacervation mechanism in engineering nano-reservoirs capable of hosting a concentrated payload of corrosion inhibitors and silver nanoparticles. Transitioning to Fig2 (B), a more intricate architecture emerges, characterized by a "Cauliflower-like" morphology where nanocapsules aggregate into dense clusters with ultra-fine diameters as low as 28.64 nm; this topography is biologically paramount as it increases surface energy and provides a nano-roughness that mimics the natural extracellular matrix of bone, thereby enhancing the ability of osteoblasts to adhere and proliferate rapidly across the implant surface. Finally, Fig2. (C) displays the most homogeneous and dense network, where the nanocapsules form a continuous protective shield devoid of micro-cracks or defects. This nano-packing serves as the direct physical explanation for the remarkable 93.75% protection efficiency observed in Tafel polarization tests, as this dense membrane effectively obstructs the infiltration of aggressive chloride ions toward the active magnesium surface. Simultaneously, these millions of nanocapsules function as "biosensors" ready to respond immediately to any pH fluctuations triggered by bacterial activity or localized corrosion. Consequently, this integrated morphological system synergistically combines the strength of a physical barrier with the intelligence of biochemical responsiveness, confirming that nano-scale surface engineering is the fundamental key to transforming the Mg-AZ31 alloy from a mere industrial metal into a smart medical implant capable of high-efficiency functional osseointegration [35].

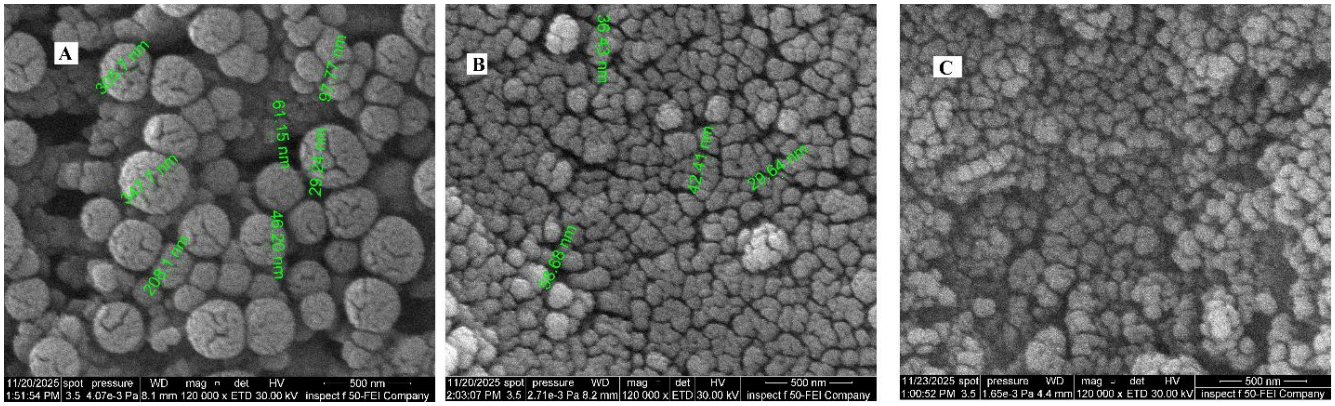


**Figure 2** Nano-interface of magnesium alloys encapsulated with MBT and silver reservoirs; images (A, B, C) show the porous structural gradient required for smart corrosion response.

### *3.3. Electrochemical analysis & results*

The Tafel polarization curves illustrated in the Figure 3 demonstrate a fundamental shift in the electrochemical degradation behavior of the Mg-AZ31 alloy following the application of the smart nanocoating. The green curve (as it is) represents the bare reference sample, exhibiting a high corrosion current and a significantly negative corrosion potential near -700 mV, confirming its excessive chemical reactivity and rapid dissolution in physiological media. However, with the integration of the nano-coating and the incremental increase in silver nanoparticle concentration (0.1,

0.2, and 0.3 AgNPs), a distinct and systematic shift of the curves toward the noble region (upward and to the left) is observed [36]. The sample with 0.3 AgNPs (red curve) achieved the superior electrochemical performance, with a corrosion potential reaching approximately -260 mV [37]. This significant positive displacement in potential, coupled with a drastic reduction in corrosion current density ($I_{corr}$), reflects the nano-system's ability to simultaneously suppress both anodic and cathodic reactions—a phenomenon known as mixed-type inhibition facilitated by the released MBT [38-40]. Consequently, this led to a stabilized reduction in hydrogen evolution and the formation of a highly resilient insulating barrier that obstructs aggressive ionic infiltration, ultimately achieving maximum protection efficiency that ensures the structural integrity of the implant for a duration sufficient for complete osseointegration [41-43].

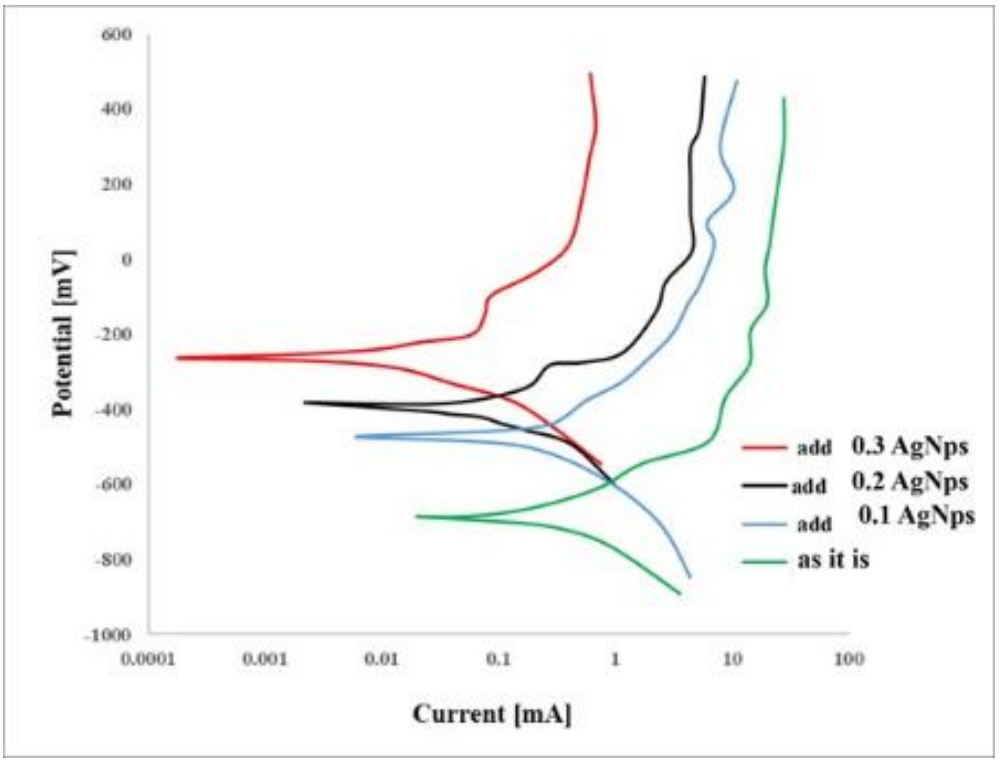


**Figure 3** Potentiodynamic polarization curves (Tafel Plots) of Mg-AZ31 alloy before and after coating with various AgNPs concentrations, demonstrating the improvement in corrosion potential and protection efficiency.

### 3.4. *Biological analysis & antibacterial results*

The results of the Zone of Inhibition (ZOI) assays presented in Figure4 (A), (B), and (C) demonstrate the exceptional biological efficacy of the smart coating system applied to the Mg-AZ31 magnesium alloy against *Staphylococcus aureus*. Figure4. (A) reveals the formation of a distinct and wide-diameter inhibitory zone surrounding the source of silver nanoparticle (AgNPs) release, indicating the high diffusivity and potent bactericidal capacity of these nanoparticles within the implant's vicinity. Figure4 (B) displays a clear gradient in bacterial density around the coated samples, validating the "Smart Release" mechanism; as bacterial metabolic activity induces a localized pH drop through acid secretion, the nanocapsules respond by swelling and partially degrading to deploy their antimicrobial payload precisely at the infection site. Furthermore, Figure4 (C) illustrates the prevention of Biofilm formation on the sample surface, maintaining a sterile bio-interface. These findings transcend mere

surface protection, confirming that the encapsulation of AgNPs within the gelatin/gum Arabic polymeric matrix provides a proactive defense line that inhibits microbial colonization. This functionality is clinically paramount in preventing peri-implantitis and ensuring successful osseointegration, thereby establishing this coating as a holistic solution that simultaneously provides chemical corrosion resistance and biological immunization against post-surgical infections.


**Figure 4** Zone of Inhibition (ZOI) results demonstrating the antibacterial efficacy against S. aureus for the coated samples, where the clear zones (A and B) indicate the potency of AgNPs ininhibiting microbial growth.

### *3.5. Cross-cut adhesion test*

The Cross-Cut Adhesion Tape Test results presented in Figure5 (A), (B), and (C) demonstrate the exceptional mechanical integrity of the engineered nanocoating on the Mg-AZ31 substrate. The inscribed grid patterns reveal a robust adherence of the polymeric layer to the metallic surface, with no signs of flaking or detachment at the edges, aligning with high-performance classifications (such as**5** B according to ASTM D3359 standards). In sample (A), the preservation of sharp square boundaries indicates strong interfacial bonding between the magnesium alloy and the polymer matrix. Meanwhile, samples (B) and (C) confirm that the integration of silver nanoparticles and nanocapsules did not compromise the mechanical properties; rather, it contributed to an interlocking network that resists crack propagation. This "Adhesive Resilience" is a critical prerequisite for clinical success, ensuring the coating can withstand surgical mechanical stresses and the physiological pressures of bone tissue regeneration. The sustained attachment of the coating ensures long-term electrochemical protection and localized corrosion resistance, providing a stable microenvironment essential for successful functional osseointegration.

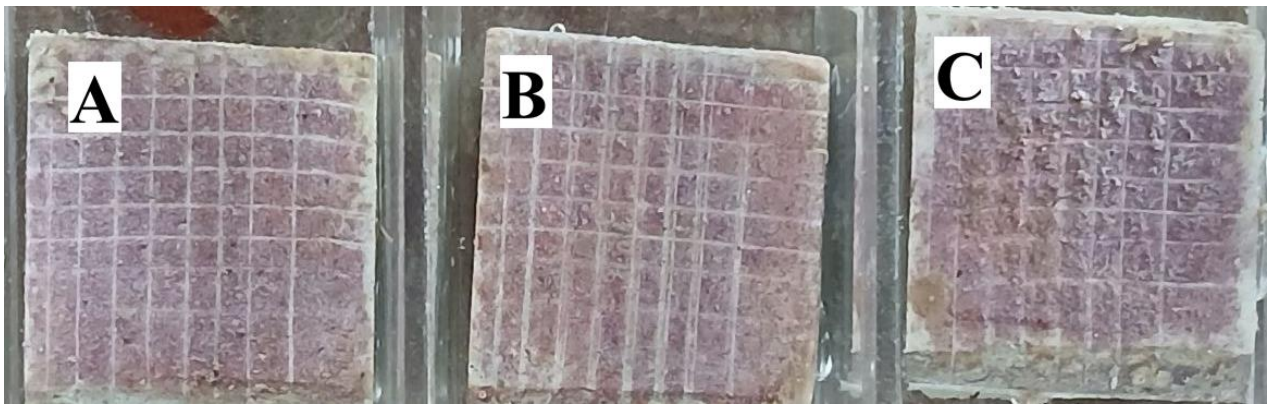


**Figure 5** Cross-cut adhesion test results of the smart coating on Mg-AZ31 alloy, demonstrating superior mechanical cohesion and zero peeling of the protective layers.

### *3.6. Effect of advanced nanotechnology on coating performance*

The integration of advanced nanotechnology significantly enhances the multifunctional performance of the coating system. Nanoscale structural control improves coating density and reduces defect pathways, thereby increasing corrosion resistance. Additionally, nanoparticle-mediated antibacterial mechanisms enhance microbial inhibition efficiency, while nano-topographical features promote cell adhesion and biointegration. These improvements demonstrate the critical role of nanotechnology in achieving simultaneous chemical, mechanical, and biological performance enhancement. Table 1 presents a comparative evaluation of conventional and nanotechnology-enhanced coating systems, demonstrating superior multifunctional performance achieved through nanoscale engineering.

**Table 1** Comparison between conventional coatings and nanotechnology-engineered smart coatings highlighting improvements in corrosion resistance, antibacterial activity, and biointegration performance.

| Parameter | Conventional Coating | Nano-Engineered Coating |
|---|---|---|
| Corrosion Resistance | Moderate | Very High |
| Antibacterial Activity | Limited | Strong |
| Surface Uniformity | Moderate | Highly uniform |
| Bioactivity | Good | Excellent |
| Smart Response | Passive | Stimuli-responsive |

Figure 6 presents the mechanisms of nanotechnology-enhanced coatings, including nanoparticle-mediated antibacterial action, corrosion inhibition, and stimuli-responsive release behavior.

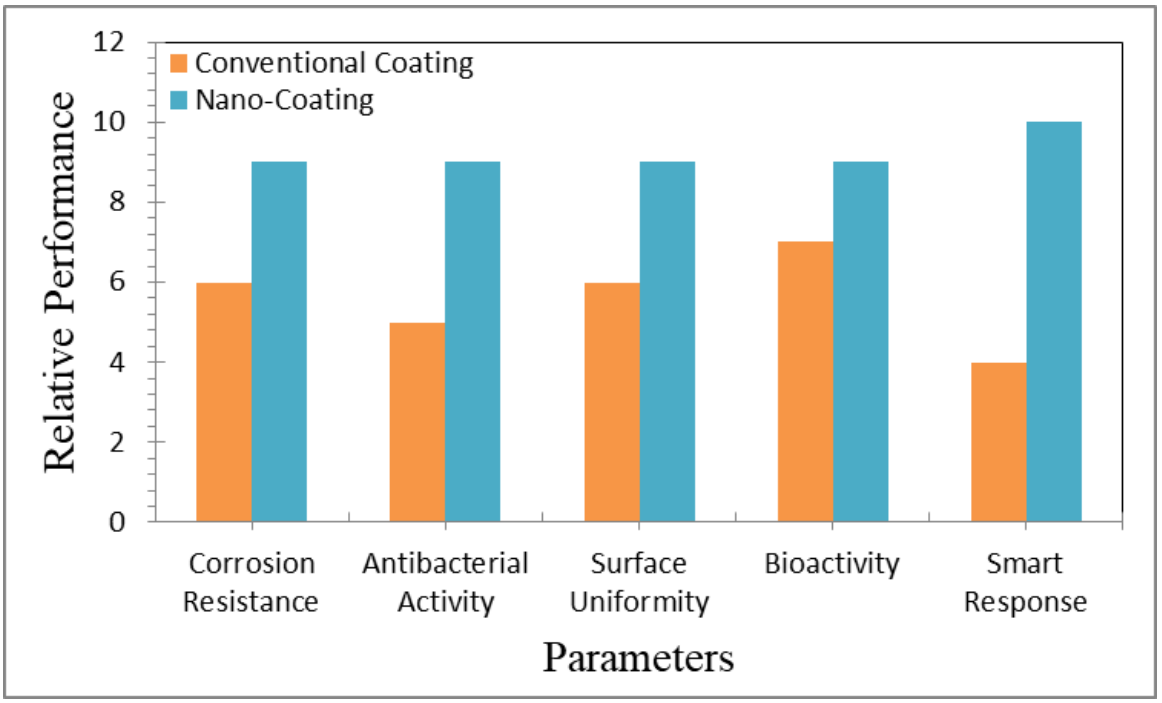


**Figure 6** Schematic illustration of nanotechnology-enhanced coating mechanisms showing nanoparticle reinforcement, smart release behavior, and biointegration processes.

## 4. CONCLUSIONS

This study successfully developed a smart, pH-responsive, and bioactive nanocoating system for Mg-AZ31 alloy, offering an integrated solution to the long-standing "magnesium paradox" in orthopedic applications. Through the design of a hierarchical nano-interface based on complex coacervation, the coating demonstrated a synergistic combination of structural stability, corrosion resistance, antimicrobial activity, and bioactivity. The FTIR analysis confirmed the formation of a stable cross-linked polymeric network, while the Cross-Cut adhesion test verified excellent interfacial bonding and mechanical integrity, ensuring the durability of the coating under physiological conditions. Electrochemical investigations revealed a significant enhancement in corrosion resistance, with a protection efficiency of 93.75%, indicating the effectiveness of the smart release mechanism. The encapsulated nanocapsules responded dynamically to pH variations, enabling the controlled release of MBT inhibitors to stabilize the electrochemical interface and suppress degradation. In parallel, biological evaluation demonstrated strong antibacterial performance against Staphylococcus aureus, where the incorporation of silver nanoparticles effectively inhibited microbial colonization and prevented biofilm formation, thereby reducing the risk of implant-associated infections. Furthermore, morphological and compositional analyses confirmed the formation of a "cauliflower-like" nanotopography, which served as a biomimetic platform for enhanced cell interaction and hydroxyapatite deposition. The observed Ca/P ratio of 1.67 indicates optimal bioactivity and supports the potential for successful osseointegration. This multifunctional behavior highlights the ability of the coating to simultaneously provide chemical protection and biological compatibility. The developed system transforms Mg-AZ31 from a highly reactive material into a self-regulating bio-platform capable of adapting to physiological conditions. The concept of "functional synchronicity" achieved in

this work ensures that the implant maintains mechanical support during the healing phase and degrades in a controlled manner thereafter. This study provides a promising pathway toward the development of next-generation biodegradable orthopedic implants that eliminate the need for secondary surgical removal while enhancing patient outcomes. The integration of advanced nanotechnology transforms conventional coatings into intelligent multifunctional systems capable of simultaneous corrosion protection, antimicrobial activity, and biointegration. Nanoscale engineering enables precise control of coating behavior, improving implant performance and reliability. Future developments in smart nanocoatings are expected to further enhance clinical outcomes and expand applications in biomedical engineering.

**References**

[1] D. Kherifi, A. Keziz, M. Rasheed, A. Oueslati. Ceram. Int. 50 (2024) 30175. https://doi.org/10.1016/j.ceramint.2024.05.317
[2] D. Kukla et al., Materials 14 (2021) 1123. https://doi.org/10.3390/ma14051123
[3] D.G. Bogard, K.A. Thole, J. Turbomach. 128 (2006) 1. https://doi.org/10.1115/1.2136291
[4] E. Arif, R. Jamal, M. RASHEED, Experimental and Theoretical NANOTECHNOLOGY, 10 (2026) 453. https://doi.org/10.56053/10.2.453
[5] E. Kadri, K. Dhahri, R. Barillé, M. Rasheed. Phase Transi. 94 (2021) 65. https://doi.org/10.1080/01411594.2020.1832224
[6] F. Boudou, A. Belakredar, A. Berkane, M. Rasheed. Not. Sci. Biol. 17 (2025) 12183. https://doi.org/10.55779/nsb17212183
[7] F. Boudou, A. Guendouzi, A. Belkredar. M. Rasheed, Not. Sci. Biol. 16 (2024) 13837. https://doi.org/10.55779/nsb16211837
[8] F. Boudou, et al., Not. Sci. Biol. 17 (2025) 12593. https://doi.org/10.55779/nsb17312593
[9] F. Dkhilalli, S. M. Borchani, M. Rasheed, R. Barille, K. Guidara, M. Megdiche, J. Mater. Sci. Mater. Electron, 29 (2018) 6297. https://doi.org/10.1007/s10854-018-8609-z.
[10] G. VanDrunen, L. Liburdi, Metall. Trans. A 9 (1978) 147. https://doi.org/10.1007/BF02646352
[11] H. A. Hussein, S. G. Hussein, and Bassim Bachy, Mathematical Modelling and Engineering Problems, vol. 12, no. 7, pp. 2234–2244, Jul. 2025, doi: https://doi.org/10.18280/mmep.120704
[12] H. K. Aity, E. Dhahri, M. Rasheed. Ceram. Int. 50 (2024) part B 54666. https://doi.org/10.1016/j.ceramint.2024.10.324
[13] H. K. Aity, M. Rasheed, E. Dhahri, A. A. Hateef, T. Saidani, Journal of Materials Science, 61 (2026) 6226. https://doi.org/10.1007/s10853-026-12241-w.
[14] H.A. Hussein et al., IOP Conf. Ser. Mater. Sci. Eng. 881 (2020) 012090. https://doi.org/10.1088/1757-899X/881/1/012090
[15] H.A. Hussein et al., IOP Conf. Ser. Mater. Sci. Eng. 987 (2020) 012014. https://doi.org/10.1088/1757-899X/987/1/012014
[16] H.A. Hussein et al., J. Mater. Eng. Perform. 32 (2022) 7149. https://doi.org/10.1007/s11665-022-07645-z
[17] H.A. Hussein et al., J. Phys. Conf. Ser. 1773 (2021) 012024. https://doi.org/10.1088/1742-6596/1773/1/012024
[18] H.L. Bernstein, Mater. Sci. Eng. A 245 (1998) 1. https://doi.org/10.1016/S0921-5093(97)00823-9
[19] I. Alshalal, H. M. I. Al-Zuhairi, A. A. Abtan, M. Rasheed, M. K. Asmail. J. Mech. Behav. Mater. 32 (2023) 1. https://doi.org/10.1515/jmbm-2022-0280
[20] I.M. Mohammed, M. Rasheed, AIP Conf. Proc. 3321 (2025) 020026. https://doi.org/10.1063/5.0289719
[21] J.C. Han, S. Dutta, S.V. Ekkad, Int. J. Heat Fluid Flow 32 (2011) 673.

https://doi.org/10.1016/j.ijheatfluidflow.2011.03.003
[22] J.R. Nicholls et al., Surf. Coat. Technol. 149 (2002) 236. https://doi.org/10.1016/S0257-8972(01)01471-3
[23] L. Meng et al., Corros. Sci. 198 (2022) 110123. https://doi.org/10.1016/j.corsci.2022.110123
[24] M. A. Sarhan, S. Shihab, B. E. Kashem, M. Rasheed, J. Phy.: Conf. Ser., 1879 (2021) 022122. https://doi.org/10.1088/1742-6596/1879/2/022122.
[25] M. Abass et al., Adv. Sci. Technol. Res. J. 17 (2023) 330. https://doi.org/10.12913/22998624/161831
[26] M. Enneffatia, M. Rasheed, B. Louati, K. Guidara, S. Shihab, R. Barillé, J. Phys.: Conf. Ser. 1795 (2021) 012050. https://doi.org/10.1088/1742-6596/1795/1/012050
[27] M. M. Najim, B. A. Yousif, M. RASHEED, Experimental and Theoretical NANOTECHNOLOGY, 10 (2026) 551. https://doi.org/10.56053/10.2.551
[28] M. M. Najim, B. A. Yousif, M. RASHEED, Experimental and Theoretical NANOTECHNOLOGY, 10 (2026) 627. https://doi.org/10.56053/10.2.627
[29] M. Modest, J. Quant. Spectrosc. Radiat. Transf. 73 (2002) 123. https://doi.org/10.1016/S0022-4073(01)00114-4
[30] M. Rasheed et al., J. Phys.: Conf. Ser. 1999 (2021) 012080. https://doi.org/10.1088/1742-6596/1999/1/012080
[31] M. RASHEED, A. Khaleefah, Materials Chemistry and Physics, 353 (2026) 132112. https://doi.org/10.1016/j.matchemphys.2026.132112.
[32] M. Rasheed, et al., J. Adv. Biotechnol. Exp. Ther. 6 (2023) 495. https://doi.org/10.5455/jabet.2023.d144
[33] M. Rasheed, I. Alshalal, A.A. Ashed, M.A. Sarhan, A.S. Jaber, Indones. J. Electr. Eng. Comput. Sci. 33 (2024) 653. https://doi.org/10.11591/ijeecs.v33.i1.pp653-660
[34] M. Rasheed, M. N. Mohammedali, F. A. Sadiq, M. A. Sarhan, T. Saidani. J. Optics (New Delhi. Print) 54 (2024) 3490. https://doi.org/10.1007/s12596-024-01928-5
[35] M. Rasheed, M. Nuhad Al-Darraji, S. Shihab, A. Rashid, T. Rashid. J. Phys.: Conf. Ser. 1963 (2021) 012058. https://doi.org/10.1088/1742-6596/1963/1/012058
[36] M. Rasheed, M.N. Al-Darraji, S. Shihab, A. Rashid, T. Rashid, J. Phys.: Conf. Ser. 1963 (2021) 012059. https://doi.org/10.1088/1742-6596/1963/1/012059
[37] M. Rasheed, O. Alabdali, S. Shihab, A. Rashid, T. Rashid, J. Phys.: Conf. Ser. 1999 (2021) 012078. https://doi.org/10.1088/1742-6596/1999/1/012078
[38] M. Rasheed, O. Alabdali, S. Shihab, J. Phy.: Conf. Ser. 1879 (2021) 032120. https://doi.org/10.1088/1742-6596/1879/3/032120
[39] M. Rasheed, O.Y. Mohammed, S. Shihab, A. Al-Adili, J. Phys.: Conf. Ser. 1795 (2021) 012043. https://doi.org/10.1088/1742-6596/1795/1/012043
[40] M. Rasheed, R. Barillé, J. Non-Cryst. Solids., 476 (2017) 1. https://doi.org/10.1016/j.jnoncrysol.2017.04.027
[41] M. Rasheed, R. Barillé, Opt. Quantum Electron. 49 (2017). https://doi.org/10.1007/s11082-017-1030-7
[42] M. Rasheed, S. Shihab, O. Alabdali, A. Rashid, T. Rashid, J. Phys.: Conf. Ser. 1999 (2021) 012077. https://doi.org/10.1088/1742-6596/1999/1/012077
[43] M. Rasheed, SuhaShihab, O. Alabdali, H. H. Hassan, J. Phys. Conf. Ser., 1879 (2021) 032113. https://doi.org/10.1088/1742-6596/1879/3/032113
[44] M. Sellam, M. Rasheed, S. Azizi, T. Saidani. Ceram. Int. 50 (2024) 20917. https://doi.org/10.1016/j.ceramint.2024.03.094
[45] M. T. Mohammed, H. A. Hussein, A. H. Lafta, Advances in Materials and Processing Technologies 1 (2025) 1. https://doi.org/10.1080/2374068x.2025.2546435

[46] M.J. Mohammed et al., J. Biomim. Biomater. Biomed. Eng. 63 (2023) 1. https://doi.org/10.4028/p-k17meg
[47] M.T. Mohammed et al., IEEE 2 (2018) 1. https://doi.org/10.1109/isces.2018.8340553
[48] N. Al-Sharify et al., Egypt. J. Chem. (2022). https://doi.org/10.21608/ejchem.2022.117967.5314
[49] N. Assoudi et al. Opt. Quant. Electron. 54 (2022) 9. https://doi.org/10.1007/s11082-022-03927-x
[50] N. Ben Azaza et al., Opt. Mater., 96 (2019) 109328. https://doi.org/10.1016/j.optmat.2019.109328
[51] N.P. Padture, M. Gell, E.H. Jordan, Science 296 (2002) 280. https://doi.org/10.1126/science.1068609
[52] O. Alabdali, S. Shihab, M. Rasheed, T. Rashid. 3rd inter. Scient. conf. alkafeel univ. (ISCKU 2021) 2386 (2022) 050019. https://doi.org/10.1063/5.0066860
[53] R. Jalal, S. Shihab, M.A. Alhadi, M. Rasheed, J. Phys.: Conf. Ser. 1660 (2020) 012090. https://doi.org/10.1088/1742-6596/1660/1/012090
[54] R.C. Reed, Acta Mater. 54 (2006) 3721. https://doi.org/10.1016/j.actamat.2006.03.047
[55] R.J. Goldstein, Int. J. Heat Mass Transf. 49 (2006) 107. https://doi.org/10.1016/j.ijheatmasstransfer.2005.07.031
[56] R.S. Mahmood et al. J. Mech. Behav. Mater. 34 (2025) 1. https://doi.org/10.1515/jmbm-2025-0040
[57] S. Kountras et al., Eng. Fail. Anal. 11 (2004) 61. https://doi.org/10.1016/S1350-6307(03)00046-1
[58] S. Lokachari et al., Surf. Coat. Technol. 474 (2024) 130107. https://doi.org/10.1016/j.surfcoat.2023.130107
[59] S. S. Batros, M. Rasheed, H. K. Aity, A. A. Hatef, T. Saidani, Materials Chemistry and Physics, 355 (2026) 132243. https://doi.org/10.1016/j.matchemphys.2026.132243
[60] S. Shihab, M. Rasheed, O. Alabdali, A.A. Abdulrahman, J. Phys.: Conf. Ser. 1879 (2021) 022120. https://doi.org/10.1088/1742-6596/1879/2/022120
[61] T. Kozhina, Procedia Eng. 100 (2015) 1290. https://doi.org/10.1016/j.proeng.2015.01.498
[62] T. Rashid, M. M. Mokji, M. Rasheed. J. Optics 54 (2024) 3490. https://doi.org/10.1007/s12596-024-02080-w
[63] T. Rashid, M.M. Mokji, M. Rasheed, J. Mech. Behav. Mater. 34 (2025) 77. https://doi.org/10.1515/jmbm-2025-0074
[64] T. Saidani, M. Rasheed, I. Alshalal, A.A. Rashed, M.A. Sarhan, R. Barillé, Res. Eng. Struct. Mater. 10 (2024) 743. http://dx.doi.org/10.17515/resm2023.21ma0922rs
[65] T. Saidani, S. Mokhtari, M. Rasheed, H. Lahmar, M. Trari, Journal of the Indian Chemical Society, 103 (2026) 102499. https://doi.org/10.1016/j.jics.2026.102499
[66] T.M. Pollock, S. Tin, J. Propuls. Power 22 (2006) 361. https://doi.org/10.2514/1.18239
[67] Y. Zhang et al., Surf. Coat. Technol. 206 (2012) 185. https://doi.org/10.1016/j.surfcoat.2011.07.047
[68] Z. Chen et al., Surf. Coat. Technol. 409 (2021) 126885. https://doi.org/10.1016/j.surfcoat.2020.126885
[69] Z. S. Ahmed, M. RASHEED, H. S. Ahmed, Experimental and Theoretical NANOTECHNOLOGY, 10 (2026) 329. https://doi.org/10.56053/10.s.329
[70] Z. S. Ahmed, M. RASHEED, H. S. Ahmed, Experimental and Theoretical NANOTECHNOLOGY, 10 (2026) 343. https://doi.org/10.56053/10.s.343
[71] A. A. Hateef, E. Dhahri, M. Rasheed, H. Kadhim, Z. Abbas, N. Hassan, Physics and Chemistry of Solid State, 25 (2024) 801. https://doi.org/10.15330/pcss.25.4.801-810
[72] A. Boumezoued, K. Guergouri, Régis Barillé, Rechem Djamil, Mourad Zaabat, M. Rasheed, J. Alloys Compd. 791 (2019) 550. https://doi.org/10.1016/j.jallcom.2019.03.251.
[73] A. Chiariotti et al., Appl. Therm. Eng. 149 (2019) 103.

[74] A. Ghoshal et al., Acta Mater. 145 (2018) 79. https://doi.org/10.1016/j.actamat.2017.11.039
[75] A. I. A. Ali, M. RASHEED, Experimental and Theoretical NANOTECHNOLOGY, 10 (2026) 277. https://doi.org/10.56053/10.s.277
[76] A. I. A. Ali, M. RASHEED, Experimental and Theoretical NANOTECHNOLOGY, 10 (2026) 239. https://doi.org/10.56053/10.s.239
[77] A. Jaber, M. Ismael, T. Rashid, M. A. Sarhan, M. Rasheed, I. M. Sala. Eureka: Phys. Eng. 4 (2023) 29. https://doi.org/10.21303/2461-4262.2023.002770
[78] A. Kanjer et al., Appl. Surf. Sci. 423 (2017) 1010. https://doi.org/10.1016/j.apsusc.2017.06.180
[79] A. Kanjer et al., Appl. Surf. Sci. 423 (2017) 1010. https://doi.org/10.1016/j.apsusc.2017.06.180
[80] A. Keziz, M. Heraiz, F. Sahnoune, M. Rasheed, Ceram. Int. 49 (2023) 32989. https://doi.org/10.1016/j.ceramint.2023.07.275
[81] A. Keziz, M. Heraiz, M. RASHEED, A. Oueslati. Mater Chem. Phys. 325 (2024) 129757. https://doi.org/10.1016/j.matchemphys.2024.129757
[82] A. Khaleefah, M. RASHEED, Experimental and Theoretical NANOTECHNOLOGY, 10 (2026) 289. https://doi.org/10.56053/10.s.289
[83] A. R. J. Katae, H. H. Hussein, A. S. Jaber, M. A. Sarhan, M. RASHEED, Experimental and Theoretical NANOTECHNOLOGY, 10 (2026) 357. https://doi.org/10.56053/10.s.357
[84] A. R. J. Katae, H. H. Hussein, A. S. Jaber, M. A. Sarhan, M. RASHEED, Experimental and Theoretical NANOTECHNOLOGY, 10 (2026) 795. https://doi.org/10.56053/10.2.795
[85] A. Raghdi, M. Heraiz, M. Rasheed, A. Keziz, Journal of the Indian Chemical Society, 101 (2024) 101413. https://doi.org/10.1016/j.jics.2024.101413
[86] A. Sheikhmohamed et al., Int. J. Heat Mass Transf. 120 (2018) 111. https://doi.org/10.1016/j.ijheatmasstransfer.2017.12.039
[87] A. Zubaidi, L.M. Asaad, I. Alshalal, M. Rasheed, J. Mech. Behav. Mater. 32 (2023) 1. https://doi.org/10.1515/jmbm-2022-0302
[88] A.D. Subhi et al., J. Min. Metall. B 58 (2022) 367. https://doi.org/10.2298/jmmb220322018s
[89] A.D. Subhi, H.A. Hussein, J. Mater. Eng. Perform. 33 (2023) 5134. https://doi.org/10.1007/s11665-023-08311-8
[90] A.G. Evans, D.R. Clarke, C.G. Levi, J. Eur. Ceram. Soc. 28 (2008) 1405. https://doi.org/10.1016/j.jeurceramsoc.2007.12.011
[91] A.H. Ali, A.S. Jaber, M.T. Yaseen, M. Rasheed, O. Bazighifan, T.A. Nofal, Complexity 2022 (2022) 1. https://doi.org/10.1155/2022/9367638
[92] A.J. Hussein, M.N. Al-Darraji, M. Rasheed, M.A. Sarhan, IOP Conf. Ser.: Earth Environ. Sci. 1262 (2023) 022007. https://doi.org/ 10.1088/1755-1315/1262/2/022007
[93] A.J. Hussein, M.N. Al-Darraji, M. Rasheed, M.A. Sarhan, IOP Conf. Ser.: Earth Environ. Sci. 1262 (2023) 022005. https://doi.org/10.1088/1755-1315/1262/2/022005
[94] A.K. Gujba et al., Wear 376–377 (2017) 1427. https://doi.org/10.1016/j.wear.2017.01.051
[95] B.R. Pai et al., J. Eng. Gas Turbines Power 107 (1985) 219. https://doi.org/10.1115/1.3239705
[96] D. Bouras, M. Rasheed, Opt. Quantum Electron. 54 (2022) 12. https://doi.org/10.1007/s11082-022-04161-1